

Feasibility Study on SPH for Application to Explosion and Structural Impact for Nuclear Safety

JinHyun Kim, Eung Soo Kim *

Department of Nuclear Engineering, Seoul National University

*Corresponding author: kes7741@snu.ac.kr

1. Introduction

In the process of nuclear power plant severe accident, steam explosion and hydrogen explosion are likely to occur and reactor containment building's exterior wall damage due to attack including aircraft impact can threaten nuclear reactor safety. However, these phenomena have many difficulties to experiment because of their danger and expensive cost.

Latest computational numerical methods can contribute to this aspect. Therefore, this study implemented an analysis model for explosion and structural impact problem by using Smoothed Particle Hydrodynamics (SPH) method and investigated the validity comparing experiment and benchmark problem results.

These phenomena involve shock waves and exist special features such as large deformations, large inhomogeneities, deformable boundaries, free surfaces and moving material interfaces. These features are generally difficult for traditional grid-based numerical methods [1]. On the contrary, a Lagrangian based meshless method SPH is easy to express large distorted condition, adopting this method to simulate both explosion and impact problem.

In this study, the SOPHIA code with changeable smoothing length algorithm and constitutive equation was used. The SOPHIA code is a GPU-parallelized SPH solver developed by Seoul National University for analyzing the complicated multi-physics problem associated with nuclear reactor safety.

2. SPH methodology

2.1 SPH approximation

The SPH method assumes the fluid system as a finite particle's group. So, a particle moves with containing their information such as mass, velocity, pressure. This information is derived by interpolation with the neighbor particle's physical variable.

The arbitrary function f 's SPH approximation is represented by multiplying the kernel function and integrating over the computational domain for a function f . For calculating numerical approximated integral formation in computer, discretized formulation is used in SOPHIA code.

$$f_i(r) = \sum_j \frac{m_j}{\rho_j} f_j W(r_i - r_j, h_i) \quad (1)$$

$$\nabla f_i(r) = \sum_j \frac{m_j}{\rho_j} f_j \nabla W(r_i - r_j, h_i) \quad (2)$$

Where i indicates center particle, j indicates neighbor particle which used in SPH approximation and m is mass, ρ is density. W is the kernel function which is a function of distance between particles and smoothing length.

The SPH derivative approximation of a function is in the similar way by multiplying the kernel function's derivative instead of kernel function. So, SPH method does not have to differentiate original function, and it has the advantage over other numerical methods.

2.2 SPH governing equation with material strength

The governing equation for hydrodynamics with material strength are the conservation equations of continuum mechanics which include the stress tensor. The stress tensor $\sigma_{\alpha\beta}$ is defined in terms of the shear stress tensor $\tau_{\alpha\beta}$ and an isotropic tensor $p\delta_{\alpha\beta}$ as follows (3).

$$\sigma_{\alpha\beta} = -p\delta_{\alpha\beta} + \tau_{\alpha\beta} \quad (3)$$

Smoothing length h decides the range of interaction for each particle. General SPH uses a constant smoothing length for all particles. However, in some cases especially explosion and impact, the particle needs to have changeable smoothing length to consider unstable environment. So deciding smoothing length's value depends on density change, and it is different for each particle [2].

$$h_i \propto \left(\frac{1}{\rho_i}\right)^d \quad (4)$$

Where d is the number of dimension.

The process of determining smoothing length includes the smoothing length correction factor term. (5).

$$\Omega_i = 1 - \frac{\partial h_i}{\partial \rho_i} \sum_j m_j \frac{\partial W_{ij}(h_i)}{\partial h} \quad (5)$$

The discretized SPH formulation has various forms of governing equation. In mass conservation, there are two approaches to calculate density in the SPH method, mass summation (6) and continuity (7). In this study, the mass summation approach is used. In momentum conservation and energy conservation, these equations choose

Table I: SPH formulation for governing equation

Governing equation	SPH formulation
Mass conservation	$\rho_i = \sum_j m_j W(h_i)$ (6)
	$\frac{d\rho_i}{dt} = \frac{1}{\Omega_i} \sum_j m_j (\mathbf{v}_i - \mathbf{v}_j) \nabla_i W_{ij}(h_i)$ (7)
Momentum conservation	$\frac{d\mathbf{v}_i}{dt} = \sum_j m_j \left[\frac{\sigma_i}{\Omega_i \rho_i^2} \nabla_i W_{ij}(h_i) + \frac{\sigma_j}{\Omega_j \rho_j^2} \nabla_i W_{ij}(h_j) - \Pi_{ij} \cdot \overline{\nabla_i W_{ij}} \right]$ (8)
Energy conservation	$\frac{dE_i}{dt} = \frac{1}{2} \sum_j m_j \overline{\mathbf{v}_{ij}} \left[\frac{p_i}{\Omega_i \rho_i^2} \nabla_i W_{ij}(h_i) + \frac{p_j}{\Omega_j \rho_j^2} \nabla_i W_{ij}(h_j) + \Pi_{ij} \cdot \overline{\nabla_i W_{ij}} \right] + \frac{\tau_{\alpha\beta i} \epsilon_{\alpha\beta i}}{\rho_i}$ (9)
Equation of state	$p_i = f(\rho_i, E_i)$ (10)

symmetric form (8), (9) and adapt the search range to bigger smoothing length to obey Newton's third law. The equation of state (EOS) is a function of density and internal energy. It is different from each simulation.

To prevent unphysical oscillation, SPH method contains artificial viscosity [3]. It restrains unphysical particle penetration and reduces numerical error around the shock wave front region. The artificial viscosity is given as (11)

$$\Pi_{ij} = \begin{cases} \frac{-\alpha c_{ij} \phi_{ij} + \beta \phi_{ij}^2}{\rho_{ij}}, & \mathbf{v}_{ij} \cdot \mathbf{x}_{ij} < 0; \\ 0, & \mathbf{v}_{ij} \cdot \mathbf{x}_{ij} \geq 0. \end{cases} \quad (11)$$

Where, $\phi_{ij} = \frac{h_{ij} \mathbf{v}_{ij} \cdot \mathbf{x}_{ij}}{|\mathbf{x}_{ij}|^2 + \varphi^2}$; $c_{ij} = \frac{1}{2}(c_i + c_j)$; $\rho_{ij} = \frac{1}{2}(\rho_i + \rho_j)$; $h_{ij} = \frac{1}{2}(h_i + h_j)$; c is the speed of sound; α, β are artificial viscosity coefficient which is upon the problem and $\varphi = 0.1h_{ij}$ is included to prevent numerical divergence when two particles are overlapping.

Unlike other terms, average kernel gradient is applied to the artificial viscosity term.

$$\overline{\nabla_i W_{ij}} = \frac{1}{2} \{ \nabla_i W_{ij}(h_i) + \nabla_i W_{ij}(h_j) \} \quad (12)$$

2.3 Elastic-perfectly plastic constitutive model for solids

The elastic-perfectly plastic constitutive equation is used for the solid impact between two particles and its formulation is as follows (13)

$$\frac{d\tau_{\alpha\beta}}{dt} = 2G(\epsilon_{\alpha\beta} - \frac{1}{3}\delta_{\alpha\beta}\epsilon_{\gamma\gamma}) + \tau_{\alpha\gamma}\mathbf{R}_{\beta\gamma} + \tau_{\gamma\beta}\mathbf{R}_{\alpha\gamma} \quad (13)$$

Where G is shear modulus; $\epsilon_{\alpha\beta}$ is strain rate tensor and $\mathbf{R}_{\alpha\beta i}$ is rotation rate tensor. The strain rate tensor and the rotation rate tensor and their discretized SPH formulation are defined as

$$\epsilon_{\alpha\beta} = \frac{1}{2} \left(\frac{\partial v_\alpha}{\partial x_\beta} + \frac{\partial v_\beta}{\partial x_\alpha} \right) \quad (14)$$

$$\mathbf{R}_{\alpha\beta i} = \frac{1}{2} \left(\frac{\partial v_\alpha}{\partial x_\beta} - \frac{\partial v_\beta}{\partial x_\alpha} \right) \quad (15)$$

and

$$\epsilon_{\alpha\beta i} = \frac{1}{2} \sum_j \frac{m_j}{\rho_j} \left[\mathbf{v}_{\alpha ji} \frac{\partial W_{ij}(h_i)}{\partial x_{\beta i}} + \mathbf{v}_{\beta ji} \frac{\partial W_{ij}(h_i)}{\partial x_{\alpha i}} \right] \quad (16)$$

$$\mathbf{R}_{\alpha\beta i} = \frac{1}{2} \sum_j \frac{m_j}{\rho_j} \left[\mathbf{v}_{\alpha ji} \frac{\partial W_{ij}(h_i)}{\partial x_{\beta i}} - \mathbf{v}_{\beta ji} \frac{\partial W_{ij}(h_i)}{\partial x_{\alpha i}} \right] \quad (17)$$

The second invariant of the shear stress J_2 is defined as (18) and the von-mises stress σ_{vm} is $\sqrt{3J_2}$.

$$J_2 = \frac{1}{2} \boldsymbol{\tau}_{\alpha\beta} : \boldsymbol{\tau}_{\alpha\beta} \quad (18)$$

Plastic regime is determined by comparing σ_{vm} and yield stress σ_Y . If σ_{vm} is bigger than σ_Y , the particle is in plastic regime and the shear stress is scaled back to the yield surface.

$$\boldsymbol{\tau}_{\alpha\beta} = \begin{cases} \frac{\sigma_Y}{\sigma_{vm}} \boldsymbol{\tau}_{\alpha\beta}, & \sigma_{vm} > \sigma_Y; \\ \boldsymbol{\tau}_{\alpha\beta}, & \sigma_{vm} \leq \sigma_Y. \end{cases} \quad (19)$$

Johnson-Cook model is chosen to calculate the yield stress σ_Y . This model (20) explains strain hardening; high strain rates and thermal softening of material.

$$\sigma_y = (A + B(\epsilon_p)^n)(1 + C \ln \frac{\dot{\epsilon}_p}{\dot{\epsilon}_0})(1 - T^{*m}) \quad (20)$$

Where A, B, C, n, m is constant; ϵ_p is the effective plastic strain; $\dot{\epsilon}_p$ is effective plastic strain rate and $\dot{\epsilon}_0 = 1s^{-1}$; and T^* is the dimensionless temperature which is defined as

$$T^* = \frac{T - T_{room}}{T_{melt} - T_{room}} \quad (21)$$

Plastic strain is updated when the particle exists in plastic regime. The plastic strain's incremental is defined as (22)

$$\Delta \epsilon_p = \frac{\sigma_{vm} - \sigma_y}{3G} \quad (22)$$

2.4 The EOS of materials

The Jones-Wilkins-Lee (JWL) EOS is used to describe the pressure products of the explosive [4].

$$p = A \left(1 - \frac{\omega\eta}{R_1}\right) e^{-\frac{R_1}{\eta}} + B \left(1 - \frac{\omega\eta}{R_2}\right) e^{-\frac{R_2}{\eta}} + \omega\eta\rho_0 E \quad (23)$$

Where A , B , R_1 , R_2 , ω are the constant coefficient upon material; η is the ratio of the explosive product's density to the initial density; ρ_0 is the initial density of the explosive products; and E is the specific internal energy.

The Mie-Gruneisen EOS is used to describe the pressure of solid materials.

$$p = \frac{\rho c_0^2 (\eta - 1) [\eta - \frac{\Gamma}{2} (\eta - 1)]}{[\eta - S(\eta - 1)]^2} + \Gamma E \quad (24)$$

Where ρ is the material's density; c_0 is the material's speed of sound; η is the ratio of the density to the initial density; E is the specific internal energy; and Γ , S are the constant coefficient upon material.

3. SPH simulation of PETN detonation

3.1 Geometry and condition of PETN detonation

The detonation phenomenon is a shock wave that propagates through the explosive with a constant velocity which is called detonation velocity driven by chemical reactions initiated at the shock front as described in Fig. 1 [4].

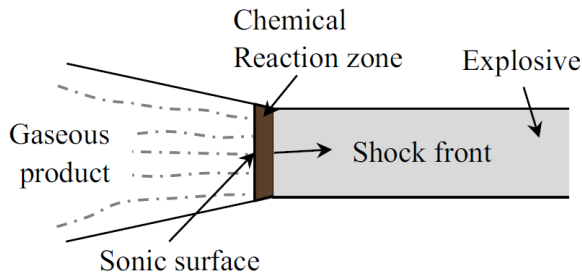


Fig. 1. Schematic of the detonation process of explosive [4]

In this study, Pentaerythritol Tetranitrate (PETN) explodes and the shock wave propagates outward. The length of the PETN slab is 0.1 m.

3.2 SPH simulation results of PETN detonation

In this case, initial particle space Δx is 5×10^{-5} m; smoothing length is $1.5\Delta x$; time step Δt is 1×10^{-9} s and artificial viscosity coefficient α , β are 1.0 and 10.0 per each.

In detonation process, pressure skyrocketed during chemical reaction and reached peak pressure P_{CJ} at reaction zone. Others study set peak pressure as experimental $P_{CJ} = 33.5$ GPa. On the contrary, the detonation result by SOPHIA set peak pressure as theoretical $P_{CJ} = 30.4$ GPa. At the unreacted zone, pressure plunged to 0.

Other properties such as density and specific internal energy also showed similar profile shape.

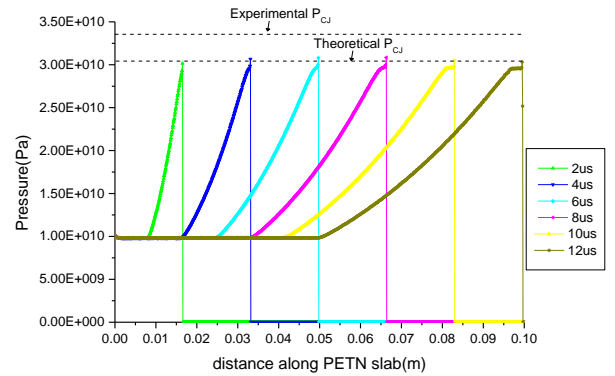


Fig. 2. Pressure profile during PETN detonation by SOPHIA code.

Table II: Coefficient of the JWL model and property for PETN

Symbol	Meaning	Value
ρ_0	Initial density	1765 kg/m^3
E_0	Initial specific internal energy	$5.722 \times 10^6 \text{ J/kg}$
D	Detonation velocity	8300 m/s
A	JWL coefficient	617 GPa
B	JWL coefficient	16.926 GPa
R_1	JWL coefficient	4.4
R_2	JWL coefficient	4.4
ω	JWL coefficient	0.25

4. SPH simulation of HVI simulation

3.1 Geometry and condition of HVI

Hyper-Velocity Impact (HVI) and its resulting penetration are representative problem of solids under extreme situation which behave like fluids [1]. When the projectile is shot toward the plate, if impact by the projectile is strong enough, the plate penetration occurs, and it causes production of debris cloud and crater.

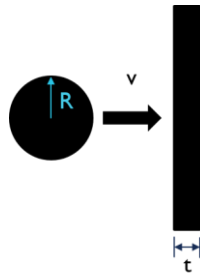


Fig. 3. Hyper Velocity Impact Geometry

In this study, Aluminum is used both sphere and plate. The sphere's radius is 0.005 m; plate's thickness is 0.004 m; and initial velocity of sphere is 6180 m/s. This condition is the same as experimental data from [5].

3.2 SPH simulation results of HVI

In this case, initial particle space Δx is 5×10^{-4} m; smoothing length is $1.2\Delta x$; time step Δt is 1×10^{-8} s and artificial viscosity coefficient α , β are both 1.5.

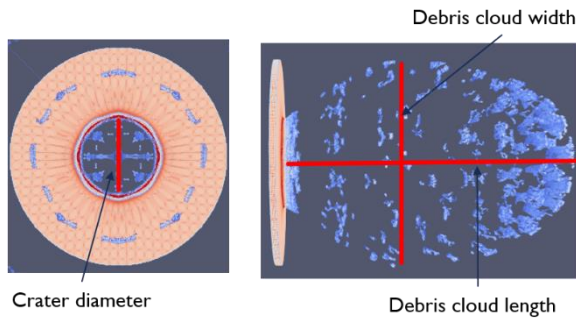


Fig. 4. Crater diameter and debris cloud's aspect ratio

To compare the results between experiment and numerical results, crater diameter; debris cloud length and debris cloud width were measured at 20 μ s. In experiment data, instead of giving the debris cloud width and length, the ratio of debris cloud length to width which is called aspect ratio is given. Crater diameter of SOPHIA code result showed an error within 10%; debris cloud aspect ratio of SOPHIA code result showed an error within 5%. The crater diameter was measured shorter and the aspect ratio suited well compared to other numerical results.

Table III: Comparison of characteristic variables among experiment and numerical simulation

	Crater diameter [cm]	Debris cloud aspect ratio
Experiment [5]	3.1	1.39
Hiermaier [5]	3.5	1.11
Chin [6]	2.89	1.22
Zhou [7]	3.345	1.36
Mehra [8]	2.4-3.2	1.53-1.9
Zhang [9]	2.85	1.344

SOPHIA	2.8	$1.328 \left(\frac{9.3 \text{ cm}}{7 \text{ cm}} \right)$
--------	-----	--

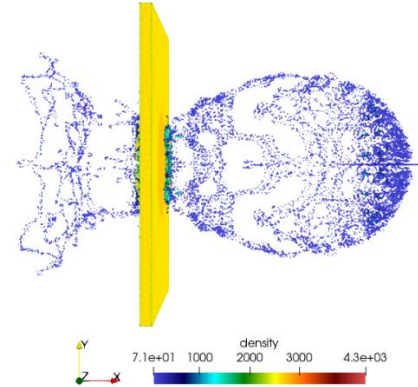


Fig. 5. HVI problem Particle distribution of SOPHIA code at 20 μ s

Table IV: Coefficient of the Mie-Gruneisen model, Johnson-Cook model and property for Aluminum

Symbol	Meaning	Value
ρ_0	Initial density	2710 kg/m ³
c_0	Speed of sound	208 m/s
G	Shear modulus	27.6 GPa
S	Mie-Gruneisen coefficient	1.5
Γ	Mie-Gruneisen coefficient	1.7
A	Johnson-Cook coefficient	175 MPa
B	Johnson-Cook coefficient	380 MPa
C	Johnson-Cook coefficient	0.0015
n	Johnson-Cook coefficient	0.34
m	Johnson-Cook coefficient	1.0
T_{room}	Reference temperature	273 K
T_{melt}	Melting point	875 K

5. Summary

SPH has an advantage over the existing grid-based method in analyzing problems accompanied by large deformations such as explosion and structure impact. In addition, the accuracy of the analysis can be further improved by adjusting the smoothing length to suit the particle's local condition. The SOPHIA code which is developed by Seoul National University demonstrates that the detonation caused by the explosion and the hyper velocity impact phenomenon are well analyzed. The detonation result showed that it reached theoretical C-J pressure, so it is worth comparing other study which reaches experimental C-J pressure. The HVI result

showed that the crater diameter was slightly shorter and the aspect ratio of debris cloud was more accurate than other study. Furthermore, it can be helpful in simulating the explosion and its resulting impact phenomena inside and outside the reactor vessel and containment.

ACKNOWLEDGEMENT

This work was supported by the Defense Research Laboratory Program of the Defense Acquisition Program Administration and the Agency for Defense Development of Republic of Korea.

REFERENCES

- [1] G.R. Liu, M.B. Liu, Smoothed Particle Hydrodynamics A Meshfree Particle Method, World Scientific, 2003.
- [2] D.J. Price, J.J. Monaghan, Smoothed Particle Magnetohydrodynamics II. Variational principles and variable smoothing length terms, Monthly Notices of Royal Astronomical Society, Vol.347, p. 139-152, 2004.
- [3] J.J. Monaghan, An Introduction to SPH, Computer Physics Communications, Vol.48, pp. 89-96, 1988.
- [4] R. Pramanik, D. Deb, Implementation of Smoothed Particle Hydrodynamics for Detonation of Explosive with Application to Rock Fragmentation, Rock Mechanics and Rock Engineering, Vol.48, pp. 1683-1698, 2015.
- [5] Hiermaier et al., Computational Simulation of the Hypervelocity Impact of Al-spheres on Thin Plates of Different Materials, International Journal of Impact Engineering, Vol.20, pp. 363-374, 1997.
- [6] G.L. Chin et al., Smoothed Particle Hydrodynamics and Adaptive Smoothed Particle Hydrodynamics with Strength of Materials, National University of Singapore, 2001.
- [7] C.E. Zhou, G.R. Liu, K.Y. Lou, Three-dimensional Penetration Simulation using Smoothed Particle Hydrodynamics, International Journal of Computational Methods, Vol.4, pp. 671-691, 2007.
- [8] V. Mehra, S. Chaturvedi, High Velocity Impact of Metal Sphere on Thin Metallic Plates: A Comparative Smooth Particle Hydrodynamics Study, International Journal of Computational Methods, Vol.4, pp. 671-691, 2007.
- [9] Z.L. Zhang, M.B. Liu, Smoothed Particle Hydrodynamics with Kernel Gradient Correction for Modeling High Velocity Impact in two- and three-dimensional Spaces, Engineering Analysis with Boundary Elements, Vol.83, pp. 141-157, 2017.